CONF-780650--6

MASTER

ULTRASONIC CHARACTERIZATION OF AUSTENITIC WELDS*

By acceptance of this article, the publisher or recipient acknowledges the U.S. Government's right to retain a nonexclusive, royalty-free license in and to any copyright covering the article.

L. Adler, K. V. Cook and D. W. Fitting
Metals and Ceramics Division
Oak Ridge National Laboratory
Oak Ridge, Tennessee 37830

ABSTRACT

Nondestructive evaluation of austenitic stainless steel weld metal is a very difficult problem. Mechanical anisotropy appears to be a major contribution and is caused by preferred local orientation of elongated subgrains and preferred crystallographic orientation. The result of this anisotropy is the directional dependence of the ultrasonic velocities (shear and longitudinal) and ultrasonic attenuation. The directional dependence of these ultrasonic parameters causes large errors in locating and sizing flaws in welds. Initial studies were carried out in a type 308 stainless steel electroslag weld to characterize this anisotropy. The apparent symmetry in the macrostructure of the electroslag weld leads us to expect orthotropic symmetry in elastic constants. A technique was developed to measure variations in velocity and attenuation with direction. The velocity data compared favorably to theoretical calculations using this orthotropic model. From the velocity data all elastic constants and engineering constants for this weld were determined. Studies of other types of welds showed that orthotropic symmetry is typical of austenitic welds. Data will be presented to show how anisotropy affects defect location and sizing in welds.

INTRODUCTION

The inspection of austenitic steels with welded or cast structures using ultrasonic techniques is often of limited value. Inspectability can vary on

---

*Research sponsored by the Division of Reactor Research and Technology, U.S. Department of Energy, under contract W-7405-eng-26 with Union Carbide Corporation.

NOTICE
This report was prepared as an account of work sponsored by the United States Government. Neither the United States nor the United States Department of Energy, nor any of their employees, nor any of their contractors, subcontractors, or their employees, makes any warranty, express or implied, or assumes any legal liability or responsibility for the accuracy, completeness or usefulness of any information, apparatus, product or process disclosed, or represents that its use would not infringe privately owned rights.

DISTRIBUTION OF THIS DOCUMENT IS UNLIMITED

DISCLAIMER

This report was prepared as an account of work sponsored by an agency of the United States Government. Neither the United States Government nor any agency Thereof, nor any of their employees, makes any warranty, express or implied, or assumes any legal liability or responsibility for the accuracy, completeness, or usefulness of any information, apparatus, product, or process disclosed, or represents that its use would not infringe privately owned rights. Reference herein to any specific commercial product, process, or service by trade name, trademark, manufacturer, or otherwise does not necessarily constitute or imply its endorsement, recommendation, or favoring by the United States Government or any agency thereof. The views and opinions of authors expressed herein do not necessarily state or reflect those of the United States Government or any agency thereof.

DISCLAIMER

Portions of this document may be illegible in electronic image products. Images are produced from the best available original document.

apparently identical specimens; therefore, we initiated some basic studies in an attempt to correlate theoretical and experimental results for nondestructive testing. This paper describes some of the work done at Oak Ridge National Laboratory to gain an understanding of the basic weld structure and its effects on ultrasonic inspectability and flaw characterization.

In austenitic stainless steels, grain growth is easy in the [001] direction and, consequently, when randomly oriented grains in base material begin to grow into fused metal, competitive growth processes favor crystals oriented in the [001] direction, parallel to the solidification direction (Fig. 1). The microstructure within a short distance from the fusion line consists predominantly of elongated grains having the favorable growth orientations and having boundaries and subboundaries parallel to the local solidification direction. These factors produce mechanical anisotropy in the stress-strain relationship. Consequently, both velocity and attenuation of the ultrasonic wave through such material will be direction dependent. The objective of this paper is (a) to model the anisotropy for welds, (b) to test the model by ultrasonic techniques and (c) to show how proper weld characterization can lead to better ultrasonic inspectability.

THEORY

Ultrasonic Wave Propagation in Anisotropic Solids with Orthotropic Symmetry

The apparent symmetry in the macrostructure of an austenitic stainless steel weld suggested the assumption of orthotropic symmetry for the stress-strain relationship. The general relation of stress to strain in matrix notation is

$$\{\sigma\} = [C]\{\varepsilon\} \qquad (1)$$

where $\{\sigma\}$ is the stress matrix, $\{\varepsilon\}$ is the strain matrix and $[C]$ is the elastic stiffness matrix. For a material with orthotropic symmetry there are nine independent terms in $[C]$:

$$[C] = \begin{bmatrix} C_{11} & C_{12} & C_{13} & 0 & 0 & 0 \\ C_{12} & C_{11} & C_{13} & 0 & 0 & 0 \\ C_{13} & C_{13} & C_{33} & 0 & 0 & 0 \\ 0 & 0 & 0 & C_{44} & 0 & 0 \\ 0 & 0 & 0 & 0 & C_{55} & 0 \\ 0 & 0 & 0 & 0 & 0 & C_{66} \end{bmatrix} \qquad (2)$$

The relationship between the elastic stiffness constants and the velocity of the ultrasonic wave is expressed by the Christoffel relation:

$$\begin{vmatrix} \lambda_{11} - \rho V^2 & \lambda_{12} & \lambda_{13} \\ \lambda_{12} & \lambda_{22} - \rho V^2 & \lambda_{23} \\ \lambda_{13} & \lambda_{23} & \lambda_{33} - \rho V^2 \end{vmatrix} = 0 \ , \qquad (3)$$

where, for a material with orthotropic symmetry

$$\begin{aligned} \lambda_{11} &= \ell^2 C_{11} + m^2 C_{66} + n^2 C_{55} \\ \lambda_{12} &= \ell m (C_{12} + C_{66}) \\ \lambda_{13} &= n\ell (C_{13} + C_{55}) \\ \lambda_{22} &= \ell^2 C_{66} + m^2 C_{22} + n^2 C_{44} \\ \lambda_{23} &= mn (C_{44} + C_{23}) \\ \lambda_{33} &= \ell^2 C_{55} + m^2 C_{44} + n^2 C_{33} \end{aligned} \qquad (4)$$

where ℓ, m and n are direction cosines of the propagation direction and ρ is the density of the material. The coordinate system attached to the weld is defined as shown in Fig. 2. Elements of the elastic stiffness matrix are calculated from measurement of sound velocity in a number of specified directions by application of the following relations.

Table 1. Relationships Between Elastic Stiffness and Ultrasonic Propagation Velocity

Propagation Direction	Elastic Stiffness Relations*
1 axis	$C_{11} = \varrho V_{11}^2, C_{66} = \varrho V_{12}^2, C_{55} = \varrho V_{13}^2$
2 axis	$C_{22} = \varrho V_{22}^2, C_{66} = \varrho V_{21}^2, C_{44} = \varrho V_{23}^2$
3 axis	$C_{33} = \varrho V_{33}^2, C_{55} = \varrho V_{31}^2, C_{44} = \varrho V_{32}^2$
1′ axis (Rotation around 3)	$C_{12} = l^{-1}m^{-1}[(l^2C_{11} + m^2C_{66} - \varrho V'^2_{11})(l^2C_{66} + m^2C_{22} - \varrho V'^2_{11})]^{1/2} - C_{66}$
2′ axis (Rotation around 1)	$C_{23} = m^{-1}n^{-1}[(m^2C_{22} + n^2C_{44} - \varrho V'^2_{22})(m^2C_{44} + n^2C_{33} - \varrho V'^2_{22})]^{1/2} - C_{44}$
3′ axis (Rotation around 2)	$C_{13} = n^{-1}l^{-1}[(n^2C_{11} + l^2C_{55} - \varrho V'^2_{33})(n^2C_{55} + l^2C_{33} - \varrho V'^2_{33})]^{1/2} - C_{55}$

[a]The first subscript on V indicates the direction of propagation and the second subscript indicates the polarization; e.g., V_{31} represents shear velocity propagating in the 3-direction and polarized along the 1-direction. Once the elastic constants are calculated from the relations above, the last three equations can be solved to calculate the variations of the velocities as a function of orientation.

EXPERIMENTAL SYSTEM

An apparatus developed to measure variation of velocity with direction in structured materials is illustrated in Fig. 3. A cylindrical sample (mounted on a goniometer) is slowly rotated about its axis. Ultrasound is transmitted through the sample on a fixed-distance path from transmitter to receiver. The signal transmitted through the sample is displayed on an oscilloscope, and the variation of velocity is measured by noting the time shift of the ultrasonic waveform. The system is aligned using an aluminum reference cylinder. This technique is capable of detecting velocity variations on the order of 1%.

Three cylindrical samples and a cubical sample (Fig. 4) are machined from the weld. The three cylinders are selected such that their axes lie along the coordinate axes. The cylinders are used for measurement of the velocity changes with orientation. By rotating each sample about its axis, continuous data may be obtained for longitudinal velocity as a function of orientation in the three orthogonal planes. For example, by rotating the sample about its 2-axis one can obtain not only V_{11} and V_{33}, but also V_{33}' (see Table 1) which is required for calculation of the elastic constants. A cube is also fabricated from the weld. Contact longitudinal and shear velocity measurements made on this sample are necessary to convert the relative velocities determined from the cylindrical samples to absolute velocities.

EXPERIMENTAL RESULTS

Two different types of weld material were available: (1) an electroslag single-pass weld of 308 stainless steel and (2) an Inconel 82 multi-pass weld (47 passes). Plots of theoretical and experimental velocity data for these two welds are given in Figs. 5 and 6. Figure 5 shows only the planes demonstrating anisotropy. The longitudinal data illustrated are obtained by through-transmission directly across the diameter of the sample. Shear-wave data were obtained from the cubical specimen. The solid curve is theoretical and is obtained by solving the last three equations from Table 1 for the primed velocities. Dots denote experimental results.

Experimental data are also presented in Figs. 7 and 8 for the variation of attenuation with orientation for the two welds. Again, plots for the single-pass weld do not include the plane of isotropy.

EFFECT OF ANISOTROPY ON SIZING DEFECTS

It has been shown before that spectra of ultrasonic waves diffracted by defects can be used for size estimation.[2,3] Figure 9 demonstrates the error which could be made in predicting the amplitude spectra of an ultasonic shear wave diffracted from a disc-shaped flaw if mechanical isotropy were assumed, when instead the material was anisotropic. The spectrum for the highest velocity shown is the true diffracted amplitude distribution when account is taken of anisotropy; that is, the distribution that would be measured. The spectrum in the foreground of the plot is that predicted from the assumption of an isotropic material. The figure dramatically demonstrates the absolute necessity of correcting for velocity variation within the weld. The greatest error results with a 45° diffracted shear wave, because of the large variations in velocity with orientation. It is ironic that this is the most commonly used angle for testing welds. It is possible to misjudge both size and location for a defect in weld by as much as 40% unless the correct procedure is followed.

SUMMARY

Mechanical anisotropy of austenitic stainless steel weld metal causes serious problems with conventional ultrasonic testing methods. A thorough characterization of these welds permits considerable improvement to be made in methods of defect location and sizing.

Analysis of the weld structure leads to the assumption of orthotropic symmetry in elastic constants. This assumption permitted the elements of the stiffness matrix to be determined from only a small number of ultrasonic velocity measurements. The elastic and engineering constants were determined for a single-pass weld of type 308 stainless steel and an Inconel 82 multipass weld. A technique developed to measure variations in velocity and attenuation with direction gave data that compared favorably to theoretical calculations using the orthotropic model.

The effects of anisotropy on sizing defects using ultrasonic frequency analysis was presented. It was found that weld characterization, with

calculation of the elastic constants and acoustic velocity, permits corrections to be made which improve sizing accuracy.

ACKNOWLEDGMENTS

The authors wish to thank R. A. Cunningham, Jr., and H. T. Murrin, Jr., for their mechanical design and fabrication contributions. We thank W. E. Deeds and W. A. Simpson for reviewing this paper. We are indebted to J. H. Bratten and other Graphic Arts personnel for their contributions. We also thank Jan Renfro of the Metals and Ceramics Division Reports Office for the typing and preparation of the paper.

REFERENCES

1. B. R. Dewey, L. Adler, R. T. King and K. V. Cook, "Measurements of Anisotropic Elastic Constants of Type 308 Stainless Steel Electroslag Welds," *Experimental Mechanics*, 17(11), 420–426, November 1977.

2. L. Adler and H. L. Whaley, "Interference Effect in a Multifrequency Ultrasonic Pulse Echo and Its Application to Flaw Characterization," *Journal of the Acoustical Society of America*, 51(3), (Pt. 2), 881–887.

3. L. Adler and D. K. Lewis, "Diffraction Model for Ultrasonic Frequency Analysis and Flaw Characterization," *Materials Evaluation*, 35(1), 51–56, January 1977.

LIST OF FIGURES

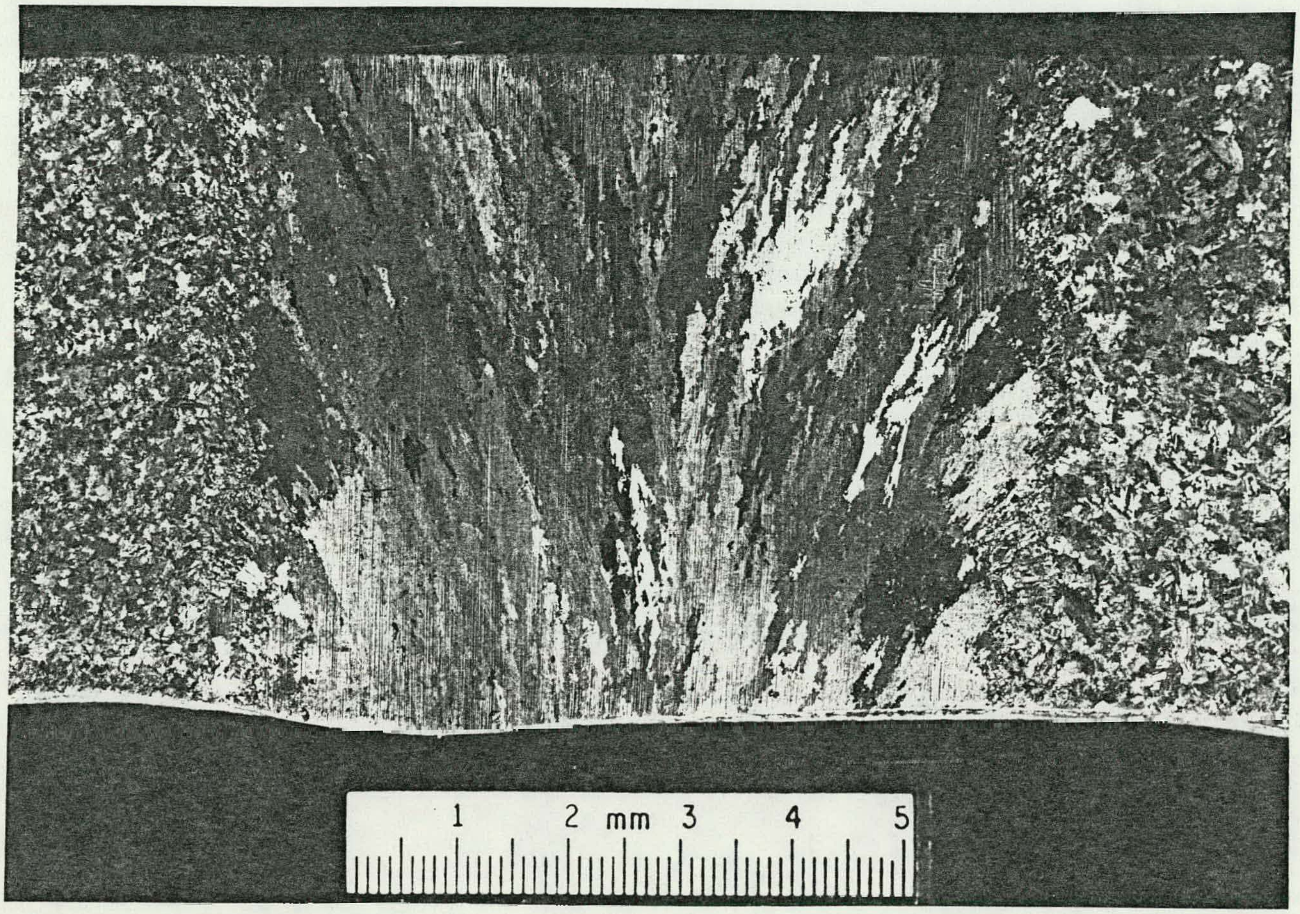

Figure 1. Macrograph of Cross Section Cut in a Plane Normal to the Hypothetical 2-axis of Fig. 2.

ORNL-DWG 75-13166R

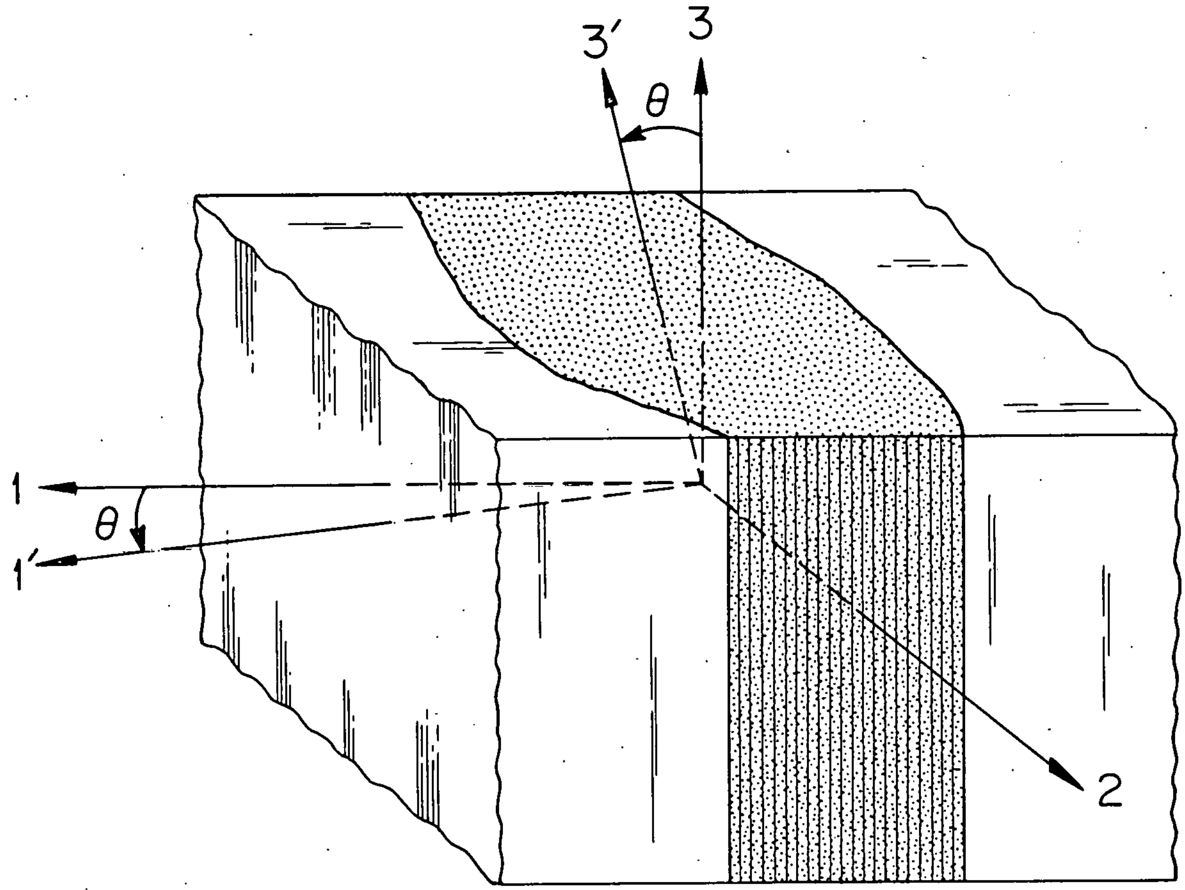

Figure 2. Idealized Electroslag Weld with Coordinate Axes. Also shown is a positive rotation around the 2 axis.

ORNL-DWG 76-19792

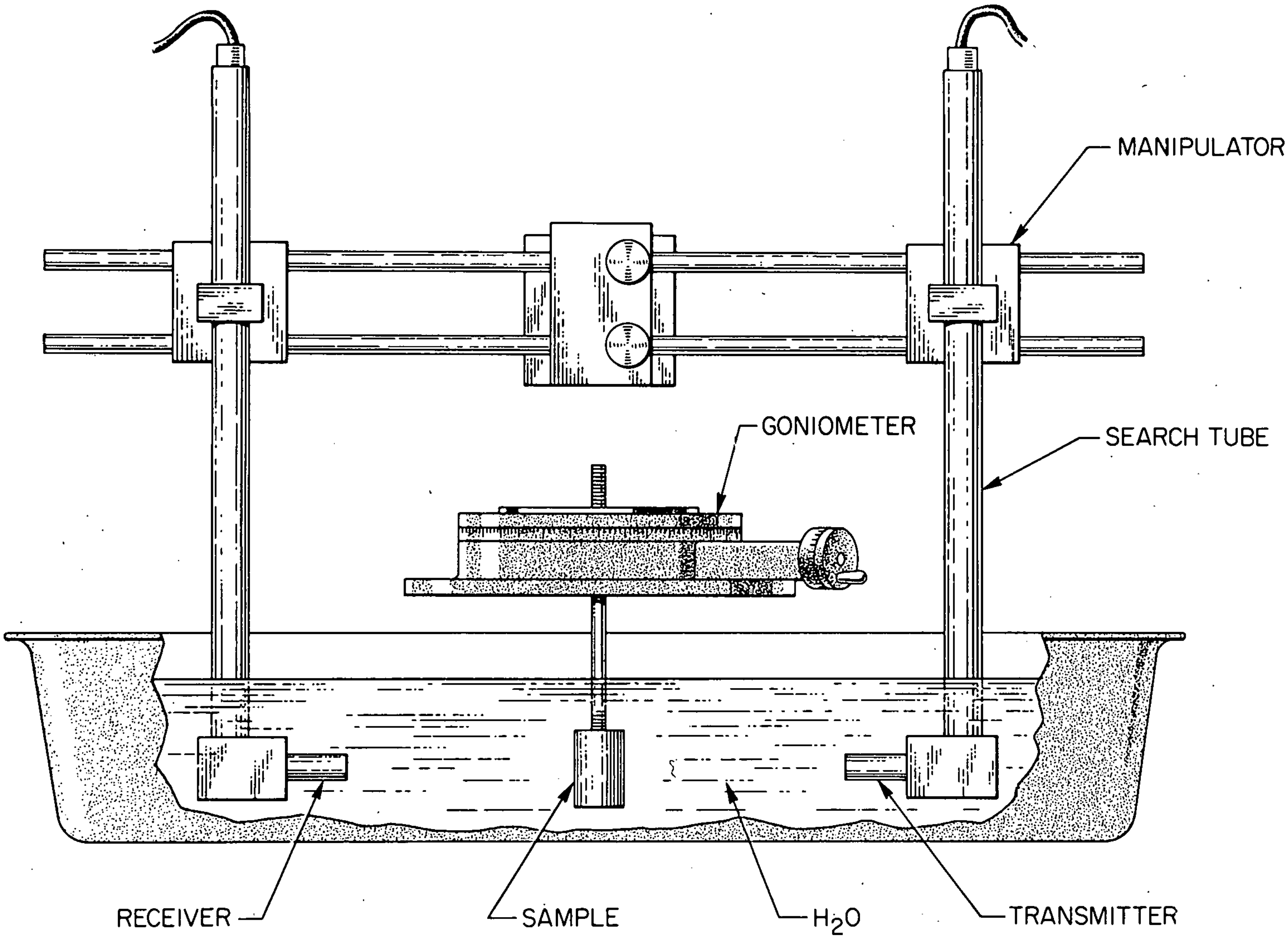

Figure 3. Apparatus for Measurement of Longitudinal Velocity Variations in a Cylindrical Sample.

ORNL-DWG 76-19793

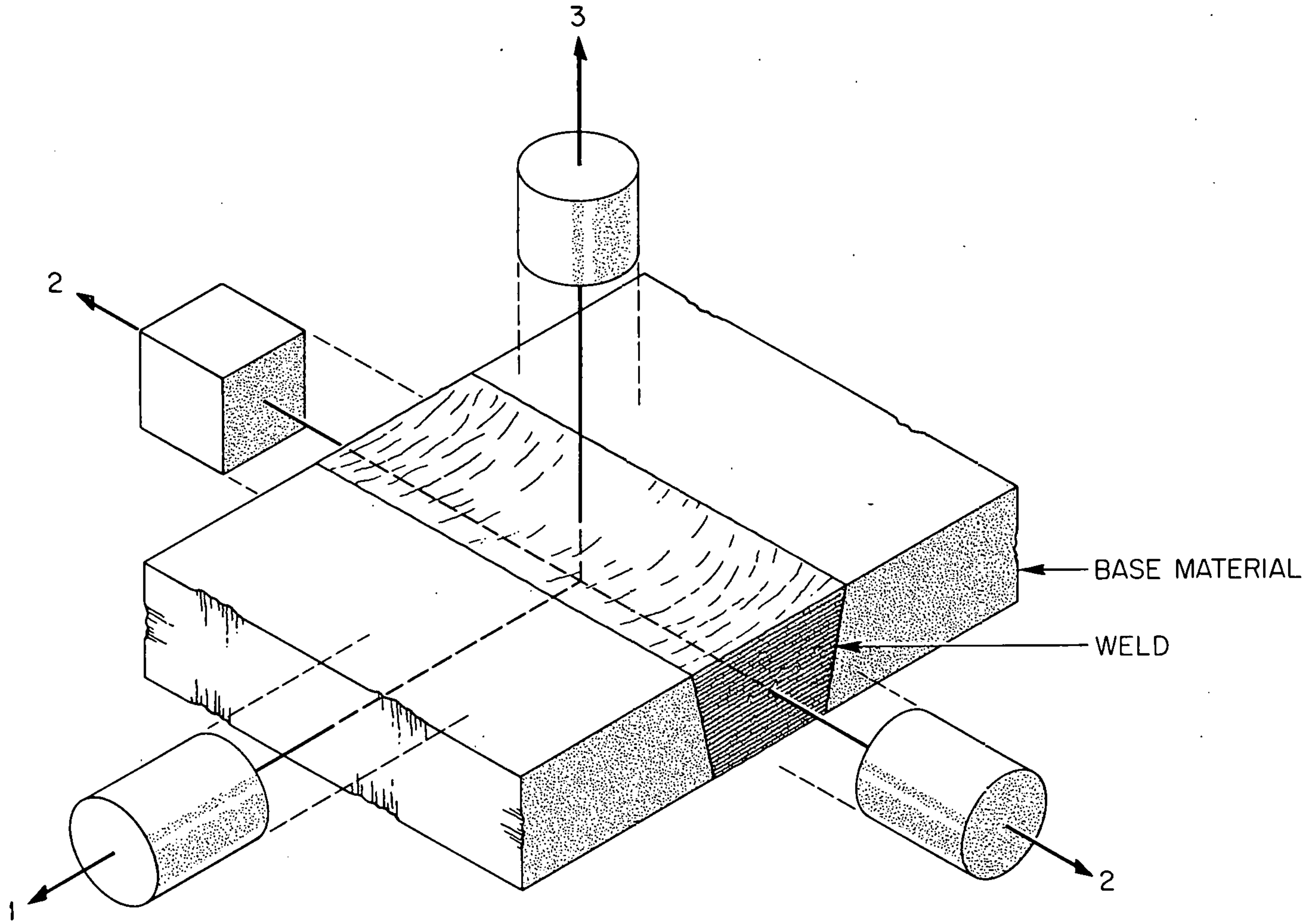

Figure 4. Sample Selection for Ultrasonic Studies from a Section of Weld.

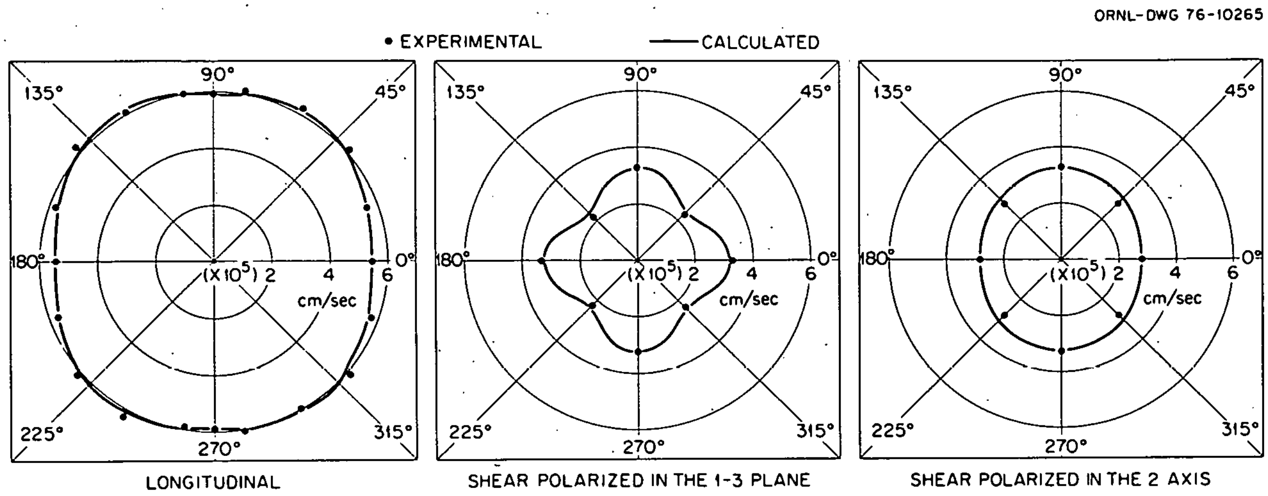

(a)

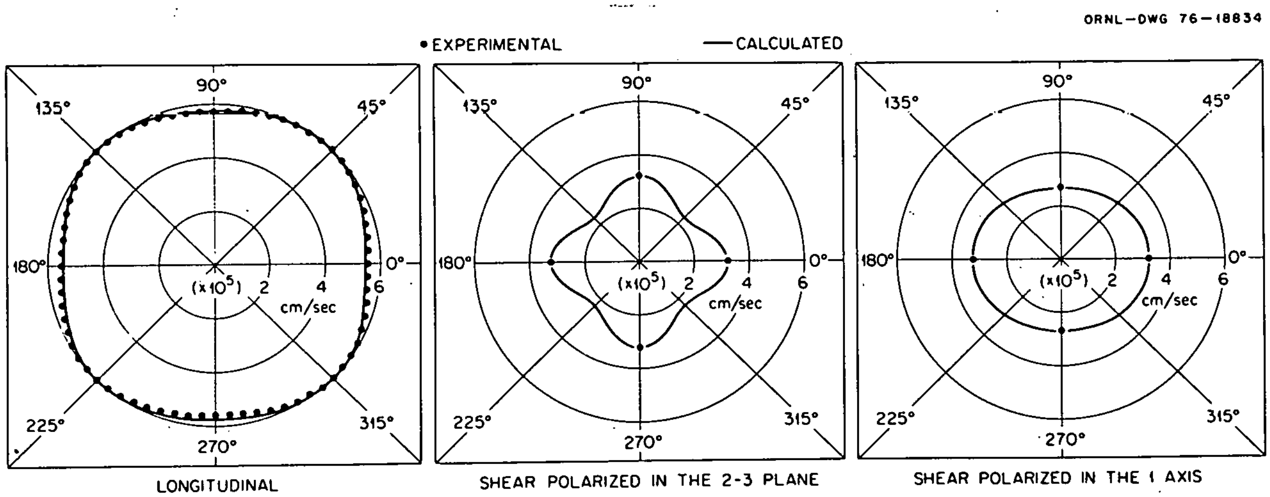

(b)

Figure 5. Anisotropic Variation of Velocity in Type 308 Stainless Steel Weld Metal. The solid curves are calculated from the Christoffel relations for the assumed orthotropic symmetry. Points are experimental. (a) In the 1–3 plant. (b) In the 2–3 plane.

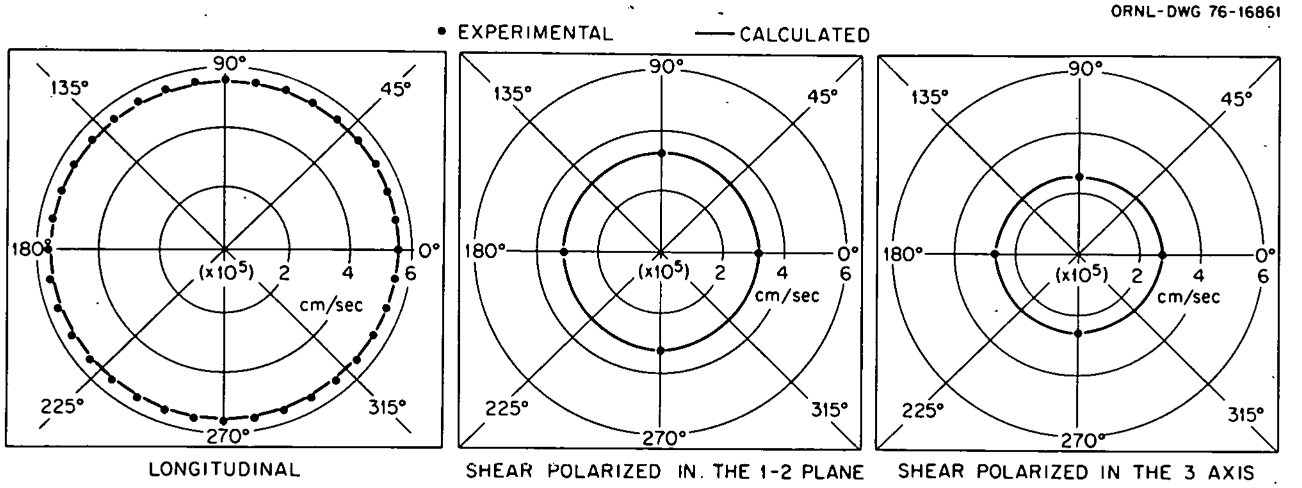

(a)

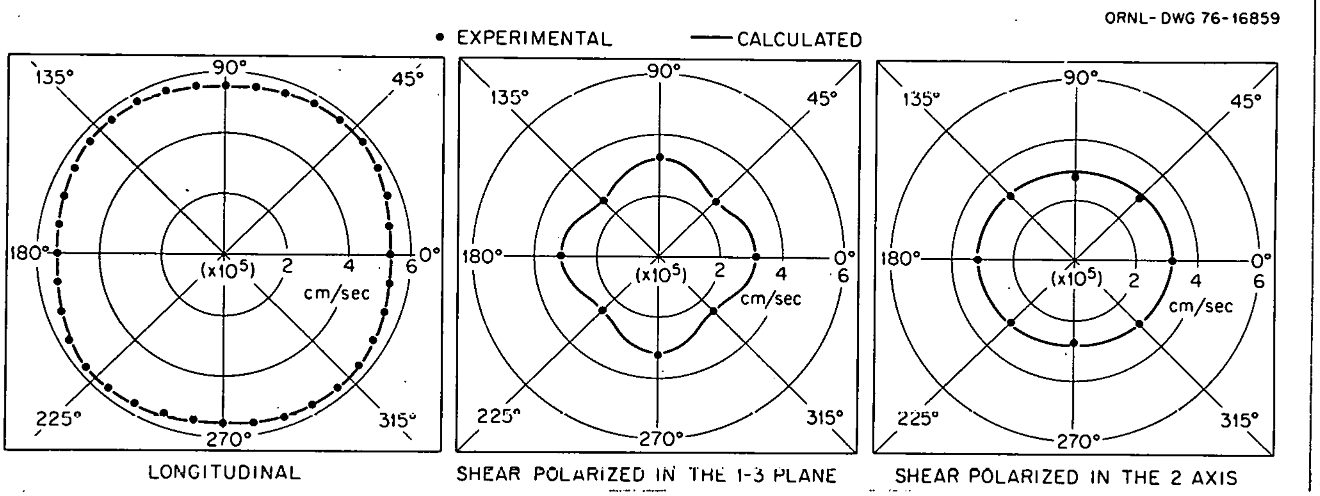

(b)

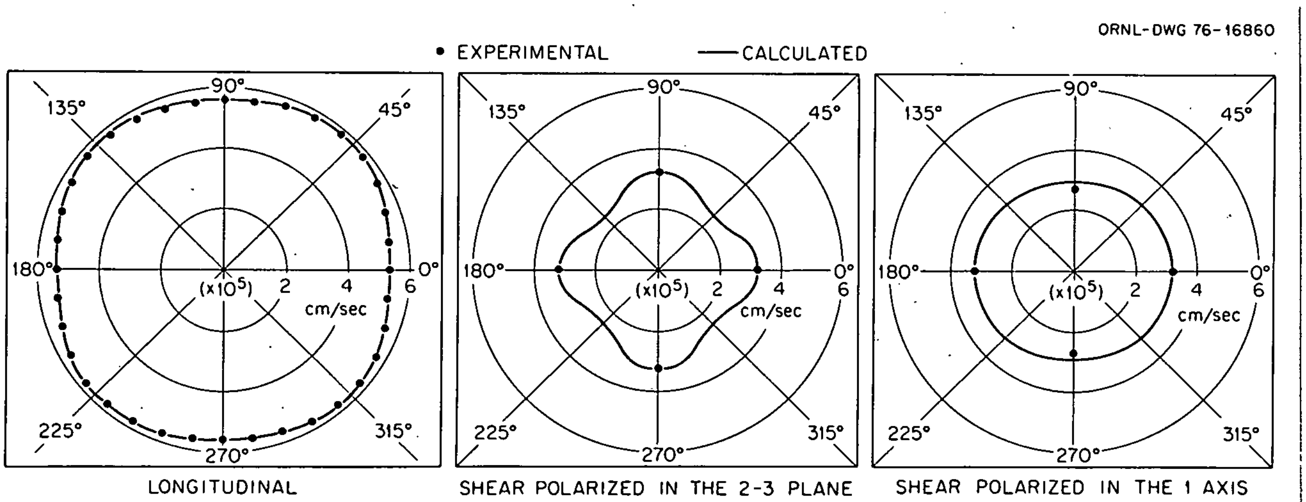

(c)

Figure 6. Variation of Ultrasonic Velocities with Orientation in a Multi-Pass Inconel 82 Weldment. The solid curves are calculated from the Christoffel relations for the assumed orthotropic symmetry. Points are experimental. (a) In 1—2 plane. (b) In 2—3 plane. (c) In 2—3 plane.

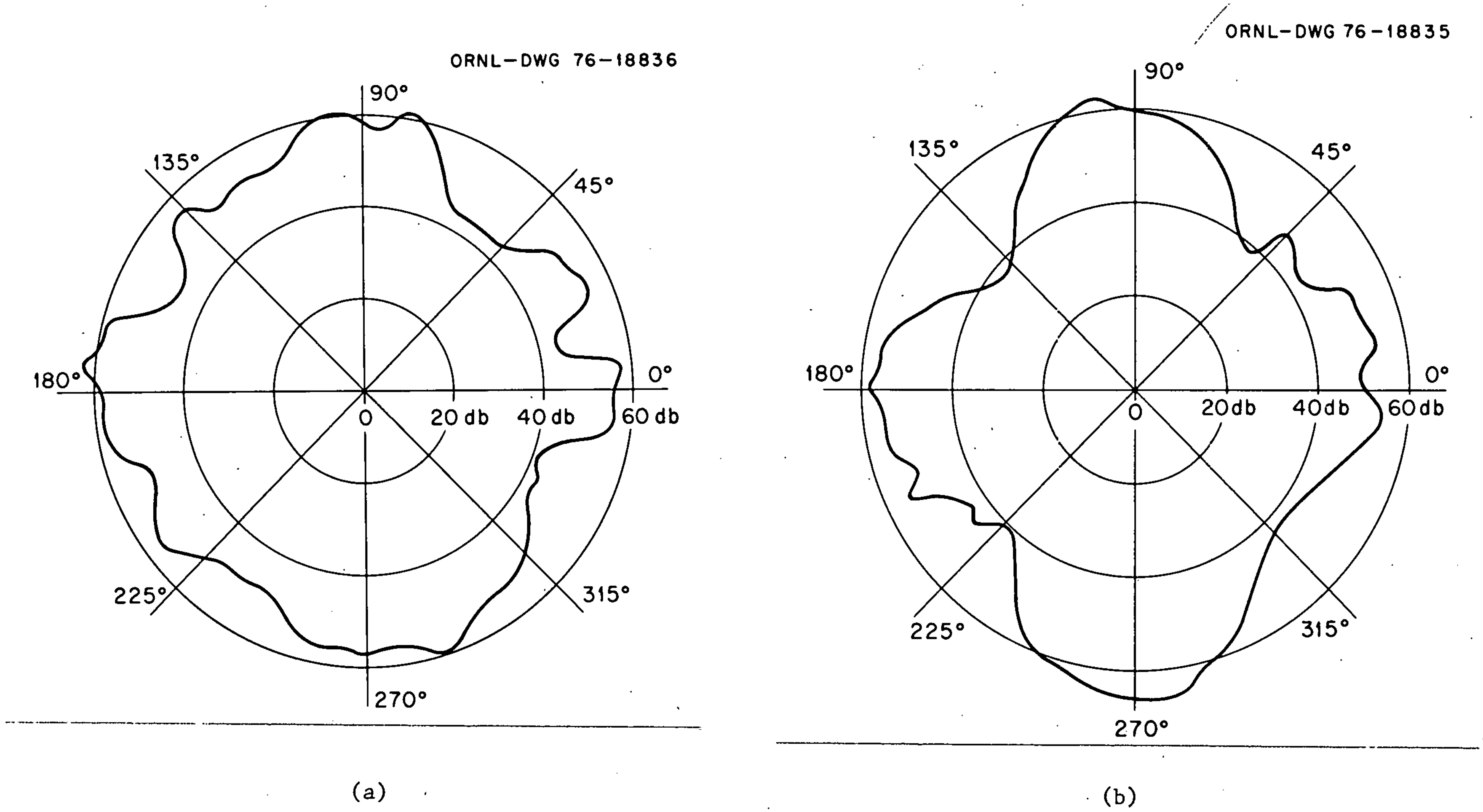

Figure 7. Variation of Relative Ultrasonic Longitudinal Wave Attenuation with Orientation in a Single-Pass Stainless Steel Weld. (a) In the 1–3 plane. (b) In the 2–3 plane.

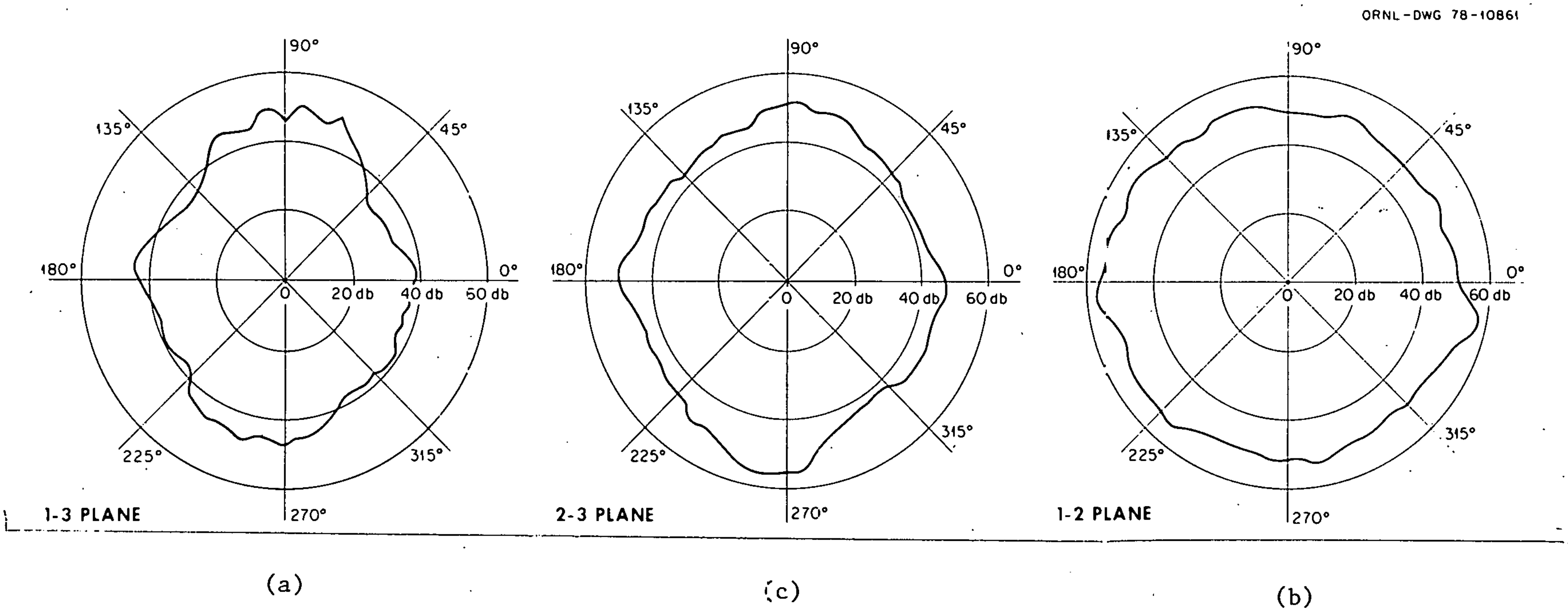

Figure 8. Variation of Relative Ultrasonic Longitudinal Wave Attenuation with Orientation in a Multi-Pass I-82 Weld. (a) In the 1–2 plane. (b) In the 1–3 plane. (c) In the 2–3 plane.

ORNL-DWG 77-3300

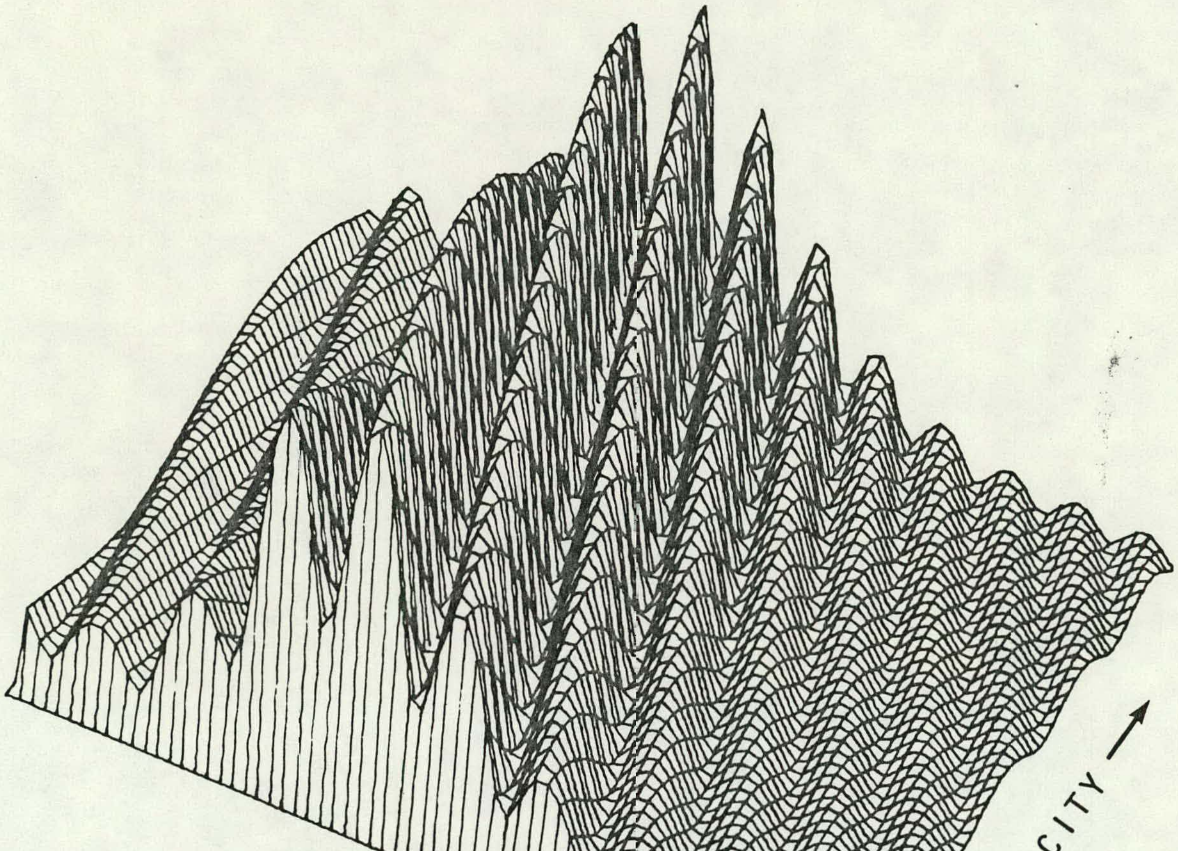

Figure 9. Effect of Anisotropy on the Amplitude Spectrum of a 45° Diffracted Shear Wave in Stainless Steel Weld Metal.